Voltage control for interconnected microgrids under adversarial actions

André Teixeira, Kaveh Paridari, Henrik Sandberg, Karl H. Johansson

***Abstract*—In this paper, we study the impact of adversarial actions on voltage control schemes in interconnected microgrids. Each microgrid is abstracted as a power inverter that can be controlled to regulate its voltage magnitude and phase-angle independently. Moreover, each power inverter is modeled as a single integrator, whose input is given by a voltage droop-control policy that is computed based on voltage magnitude and reactive power injection measurements. Under mild assumptions, we then establish important properties of the nominal linearized closed-loop system, such as stability, positivity, and diagonal dominance. These properties play an important role when characterizing the potential impact of different attack scenarios. In particular, we discuss two attack scenarios where the adversary corrupts measurement data and reference signals received by the voltage droop-controllers. The potential impact of different instances of each scenario is analyzed using control-theoretic tools, which may be used to develop methodologies for identifying high-risk attack scenarios, as is illustrated by numerical examples.**

I. Introduction

Motivated by environmental, economic and technological aspects, interests in renewable energy sources is growing worldwide. Most of these sources are small-scale inverter-based distributed generation (DG) units connected at the low voltage (LV) and medium voltage (MV) levels. Thus, the power generation infrastructure is moving from purely large centralized plants at the high voltage levels to a mixed generation pool consisting of conventional large plants and smaller distributed generation units at lower voltage levels. In this new paradigm, it is more challenging to operate the electric power networks in a reliable and resilient mode. These challenges may be tackled by facilitating a local integration of renewable energy sources, which las led to the concept of microgrids (MGs) [1], [2]. An MG is a low-voltage electrical network, composed of several DGs, energy storage elements, and controllable loads, and their integration with the main grid is accomplished by using suitable power electronic devices (inverters). In addition, an MG is able to operate in the grid-connected mode (connected to the wide-area electric power system), and also in the islanded mode (disconnected from the main grid).

Electrical power networks in the new energy generation paradigm are very complex and face numerous challenges. To facilitate their safe and reliable operation, they need to be tightly coupled with the supervisory control and data acquisition (SCADA) systems that monitor and operate the power infrastructure by collecting data from remote facilities and meters, and sending back supervisory control commands. On the other hand, the power networks coupled with the SCADA systems face new challenges, as these systems may become susceptible to malicious cyber threats through the communication infrastructure. The safe and stable operation of power networks must be ensured, not only in the normal situations, but also in the cases when the cyber security of SCADA systems is threatened by malicious attacks [3]. Thus, it is also important to analyze potential vulnerabilities of the system, by modeling and studying different threats to the controlled system, and devise resilient schemes to mitigate high-risk threats.

Recently, there has been a substantial work on cyber security of power transmission networks, addressing, for instance, certain classes of undetectable false data injection attacks [4]–[7]. In addition, the impact of these attacks on the system operation [8], [9] and possible protective and countermeasures [10], [11] have been investigated.

In comparison with transmission level, as mentioned in [12], security issues at the distribution system level have not been as extensively studied. The impact of cyber attacks on centralized voltage regulation in distribution systems was considered in [12], where a detection algorithm was proposed to mitigate the impact of sparse attacks. The vulnerabilities that may be introduced by the integrated Volt-VAR control scheme when an adversary is able to inject false data measurements into the system is studied in [13]. To the best of our knowledge, none of the previous works have studied cyber attacks on the inverter-based microgrid.

In this paper, we first tackle the problem of voltage stability and reactive power balancing in the droop-controlled MGs, and provide criteria for designing the controller gains in terms of the power system parameters. Stability and power sharing analysis of droop-controlled MGs has been carried out in several studies in the literature. For radial lossless microgrids, and under the assumption of constant voltage amplitudes, analytic conditions for proportional power sharing and synchronization of have been derived in [14]. Conditions for voltage stability for lossless parallel MGs with one common load have been derived in [15]. In addition, [16] gives conditions on the droop gains to ensure stability of droop-controlled inverter-based lossless MGs with general meshed topology. In contrast to [14]–[16] no assumptions of constant voltage amplitudes, small phase angle differences, or lossless MGs are made in this paper.

Having established relevant properties of the power system, we identify potential vulnerabilities in the interface between the physical and the IT infrastructures that may lead to an abnormal operation of the distribution network. In particular, relevant attack scenarios are introduced, together with their

threat models, based on which impact analysis are performed. The attack scenarios in this work consider cyber adversaries that may corrupt a few measurements and reference signals, which may degrade the system's reliability and even destabilize the voltage magnitudes. For example, we show that a cyber adversary, without having substantial model knowledge, may destabilize the power system by merely redirecting measurements communicated through the communication network.

The paper is organized as follows. Some definitions and known results are reviewed in Section II. The system configuration and controller structure for the inverter-based MGs are described in Section III. Conditions for the power network parameters and controller gains that ensure the system to be positive and stable are given in Section IV. Different attack scenarios against the droop-controlled MGs and preliminary results on their impact are proposed in Section V. Final remarks and conclusions are drawn in Section VI.

II. Preliminaries

In this section, we recall important properties of certain classes of linear time-invariant (LTI) systems that will be useful in the subsequent sections. Let us consider a general LTI system of the form:

$$\begin{cases} \dot{x}(t) = Ax(t) + Fu(t) \\ y(t) = Cx(t) + Du(t), \end{cases} \tag{1}$$

where $x(t) \in \mathbb{R}^n$, $u(t) \in \mathbb{R}^m$ and $y(t) \in \mathbb{R}^p$ are the system state, the control input, and the controlled output at time t, respectively. Denoting $a_{ij} = [A]_{i,j}$ as the entry of A in the i-th row and j-th column, the class of diagonally dominant matrices is defined as follows.

Definition 1 (Diagonally dominant matrices)**.** *The matrix A is said to be row-diagonally dominant if its entries satisfy the conditions*

$$|a_{ii}| \geq \sum_{j \neq i} |a_{ij}|, \ \forall i \in \{1, \ldots, n\}. \tag{2}$$

Given the above definition, the system (1) is said to be row-diagonally dominant if the state matrix A is row-diagonally dominant.

Another relevant class of systems is that of positive systems (see [17], for instance), which play an important role throughout this paper.

Definition 2 (Positive systems)**.** *The LTI system (1) is said to be positive if the following conditions hold:*

1) *The matrix A is Metzler, i.e., it has non-negative off-diagonal entries;*
2) *The matrices F, C and D are non-negative, i.e., they only have non-negative entries.*

Positive systems have several interesting properties, e.g., $x(0) \geq 0$ and $u(t) \geq 0$ result in trajectories satisfying $x(t) \geq 0$ for all t, where $x \geq 0$ for a vector x denotes the element-wise inequality. In particular, the following properties of positive systems are instrumental in our analysis.

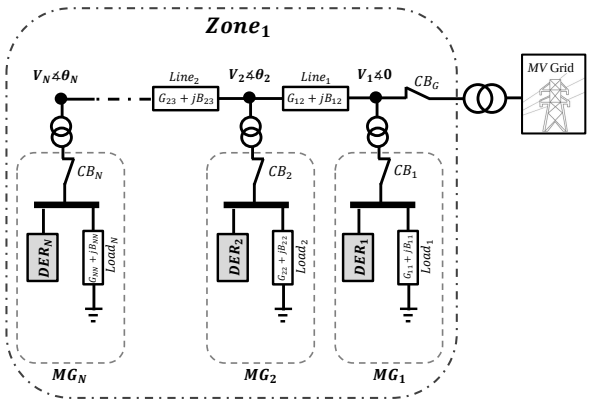

Figure 1. A power distribution system comprised of interconnected microgrids with inverter-based DERs.

Proposition 1 ([17])**.** *If the system (1) is positive, the following statements hold:*

1) *The matrix A is Hurwitz (every eigenvalue of A has strictly negative real part) if, and only if, there exists a $\xi \in \mathbb{R}^n$ such that $\xi > 0$ and $A\xi < 0$.*
2) *Let $m = p = 1$, define $H(s) = C(sI - A)^{-1}F + D$ as the transfer function of the system (1), and suppose A is Hurwitz. The $\mathcal{L}_\infty$-induced norm of (1) is given by*

$$\| H \|_{\infty - ind} = \sup_{\|u\|_{\mathcal{L}_\infty} < \infty} \frac{\| y \|_{\mathcal{L}_\infty}}{\| u \|_{\mathcal{L}_\infty}} = H(0). \tag{3}$$

III. Problem Formulation

As shown in Fig. 1, the power distribution system is considered to be a set of interconnected MGs that may be connected to the main grid through the feeder substation (bus 0), where each MG is represented by a bus to which inverter-based DER resources and loads are connected. Although Fig. 1 depicts a line network, we consider generic connected topologies where the network is characterized by the undirected graph $\mathcal{G}(\mathcal{V}, \mathcal{E})$, where $\mathcal{V}$ is the vertex set, $\mathcal{E}$ is the edge set, and $\mathcal{N}_i = \{j \in \mathcal{V} : (i,j) \in \mathcal{E}\}$ denotes the neighbor set of the i-th bus. In this system, the states are defined as V_i and θ_i, which are voltage magnitude and voltage angle of the i-th bus, respectively, and $i \in \mathcal{V}$.

Assumption 1. *In the power distribution network under study, the following assumptions are made:*

1) *The three-phase power network is balanced (so that it can be represented as an equivalent single-phase system);*
2) *All N buses are assumed to be inverter buses [2], each represented by V_i and θ_i for $i = 1, \ldots, N$.*

Under the Assumption 1, the active and reactive power injections at bus i is given respectively by

$$\begin{aligned} P_i &= V_i^2 G_i - \sum_{j \in \mathcal{N}_i} V_i V_j (G_{ij} \cos(\theta_{ij}) + B_{ij} \sin(\theta_{ij})), \\ Q_i &= -V_i^2 B_i - \sum_{j \in \mathcal{N}_i} V_i V_j (G_{ij} \sin(\theta_{ij}) - B_{ij} \cos(\theta_{ij})), \end{aligned} \tag{4}$$

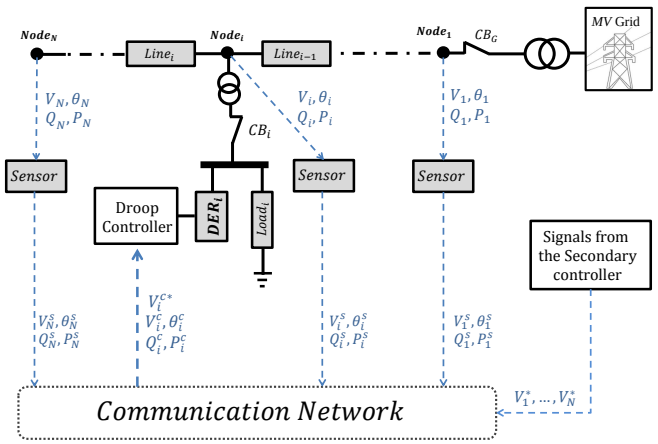

Figure 2. The inverter-based DERs of a MG are controlled by a droop controller. The physical quantities are measured by sensors at each node, which then transmit their measurements (denoted by the superscript *s*) to the droop controllers. The control signal is computed based on the measurements and reference signals received by the controller (denoted with the superscript *c*).

in which, $G_{ij} = R_{ij}/(R_{ij}^2 + X_{ij}^2) \geq 0$ and $B_{ij} = -X_{ij}/(R_{ij}^2 + X_{ij}^2) \leq 0$ are respectively the conductance and susceptance of the transmission line between the i-th and j-th buses, and R_{ij} and X_{ij} are resistance and reactance of the same line between the same buses, respectively. In addition, self-conductance and self-susceptance are defined as $G_i = G_{ii} + \sum_{j\in\mathcal{N}_i} G_{ij}$ and $B_i = B_{ii} + \sum_{j\in\mathcal{N}_i} B_{ij}$, respectively. Note that the angle difference between node i and j, $\theta_i - \theta_j$, is simply written as θ_{ij} in the rest of the paper.

Assumption 2. *In the power distribution system under study, all transmission line impedances are assumed to have the uniform ratio $\rho = R_{ij}/X_{ij} = -G_{ij}/B_{ij}$ for all $(i,j) \in \mathcal{E}$.*

A. Controller structure

Using the capabilities of the local inverter-based DERs, each MG is controlled by a droop controller, which remotely receives the reference signal (V_i^* as the reference voltage for the i-th bus) and measurements (V_j and θ_j, as the voltage magnitude and voltage angle of the j-th bus, respectively) through the communication network, using a suitable communication protocol such as the IEC 61850. The controller and related signals are shown in Fig. 2. Since we are interested in the voltage dynamics of the power system, the phase-angle dynamics are neglected and we assume that all phase-angles are constant. In terms of the voltage dynamics, each MG i is modeled as the single integrator

$$\tau_i \dot{V}_i(t) = u_{V_i}(t), \tag{5}$$

where $\tau_i > 0$ is the inverter's time constant and $u_{V_i}(t)$ is the control signal computed by the droop controller at time $t \geq 0$. In particular, we consider the voltage quadratic droop controller [14, see equation (7)] described by

$$u_{V_i}(t) = -K_i V_i^c(t)\left(V_i^c(t) - V_i^{c\star}(t)\right) - Q_i^c(t), \tag{6}$$

where $K_i > 0$ is the droop control gain and $V_i^c(t)$, $Q_i^c(t)$, and $V_i^{c\star}(t)$ are the voltage measurement, reactive injection measurement, and voltage reference signal with respect to bus i, respectively, that are received by the droop controller, as illustrated in Fig. 2.

Under nominal operation, we have that these signals match the corresponding physical variables and reference signals, i.e., $V_i^c(t) = V_i(t)$, $Q_i^c(t) = Q_i(t)$, and $V_i^{c\star}(t) = V_i^\star(t)$ ($V_i^\star(t)$ is sent by a higher level controller which is called Secondary controller). Hence, the closed-loop dynamics of inverter node i under nominal operation are given by the differential equations

$$\begin{aligned}\tau_i \dot{V}_i &= -K_i V_i\left(V_i - V_i^\star\right) - Q_i \\ &= -V_i\left(K_i V_i - K_i V_i^\star + \sum_{j\in\mathcal{V}} l_{ij}(\theta) V_j\right), \ \forall i = 1,\dots,N,\end{aligned} \tag{7}$$

where the time argument has been omitted. In addition, under the Assumption 2, the parameter l_{ij} is written as

$$l_{ij} = \begin{cases} B_{ij}(\rho\sin(\theta_{ij}) + \cos(\theta_{ij})), & i \neq j \\ -B_i, & i = j. \end{cases} \tag{8}$$

Denoting $V = [V_1 \ \dots \ V_N]^\top$ and $[V]$ as the diagonal matrix with $[V]_{ii} = V_i$, the voltage dynamics under the quadratic droop control can be written in vector form as

$$[\tau]\dot{V} = [V]\left([K]V^\star - \left([K] + L(\theta)\right)V\right), \tag{9}$$

where the matrix $L(\theta)$ is defined as $[L(\theta)]_{ij} = l_{ij}(\theta)$ and $[K]$ as the diagonal matrix with $[K]_{ii} = K_i$.

B. Linearization of the voltage dynamics

In the following sections, we consider that the power system (9) is linearized around an equilibrium point $(\bar{V}, \bar{V}^{c\star})$ such that $-\left([K] + L(\theta)\right)\bar{V} + [K]\bar{V}^\star = 0$. Additionally, the following assumptions is considered throughout the remainder of the paper.

Assumption 3. *The phase-angle differences between any neighboring nodes, θ_{ij} for $(i,j) \in \mathcal{E}$, is assumed to be constant.*

By Assumption 3, and denoting $x(t) = V(t) - \bar{V}$ and $u(t) = V^{c\star}(t) - \bar{V}^{c\star}$ as the voltage and reference deviations, respectively, the corresponding linearized system is given by

$$\dot{x}(t) = Ax(t) + Fu(t), \tag{10}$$

where $A = -[\bar{V}][\tau]^{-1}\left([K] + L(\theta)\right)$ and $F = [\bar{V}][\tau]^{-1}[K]$. For simplicity, in the following we suppose that $\bar{V} = \mathbf{1}\text{pu}$, where $\mathbf{1}$ denotes a vector with all entries equal to 1.

IV. Stability Analysis

In this section, we provide necessary and sufficient conditions on the power system parameters so that the linearized dynamics are positive and row-diagonally dominant. These properties are then used to establish the asymptotic stability of the linearized system. Moreover, they play an important role when studying the power system under the different attack scenarios in subsequent sections.

A. System properties

First we derive necessary and sufficient conditions for the linearized system (10) to be positive, which requires the following definition.

Definition 3. *The maximum phase difference between any two neighboring nodes is defined as*

$$\Delta_\theta = \max_{(i,j)\in\mathcal{E}} |\theta_{ij}|. \tag{11}$$

In addition, as in any conventional power system, here we assume that $\Delta_\theta < \pi/2$ [16].

Theorem 1. *Consider the power distribution network under study, having active and reactive power injections (4) at bus i with $\Delta_\theta < \pi/2$, and applying the quadratic droop controller (7) for each MG. Then the necessary and sufficient condition to make the linearized system (10) positive is*

$$\rho \leq |\cot(\Delta_\theta)|. \tag{12}$$

Proof. Recall the linearized system (10) with $F = [\tilde{\tau}]^{-1}[K]$ and $A = -[\tilde{\tau}]^{-1}([K] + L(\theta))$. From (8), a_{ij} read as

$$a_{ij} = \begin{cases} -\tau_i^{-1} B_{ij}(\rho\sin(\theta_{ij}) + \cos(\theta_{ij})), & i \neq j \\ \tau_i^{-1}(-K_i + B_{ii} + \sum_{j\in\mathcal{N}_i} B_{ij}), & i = j. \end{cases} \tag{13}$$

Based on Definition 2, the system is positive if and only if $[F]_{i,j} \geq 0$ and $a_{ij} \geq 0$ for all i and j. Since the controller parameters τ_i and K_i are positive, we conclude that $[F]_{i,j} \geq 0$ holds. Moreover, as the susceptance B_{ij} is always negative, the inequalities $a_{ij} \geq 0$ for all i and j can be rewritten as

$$\begin{cases} \rho\sin(\theta_{ij}) + \cos(\theta_{ij}) \geq 0 \\ \rho\sin(\theta_{ji}) + \cos(\theta_{ji}) \geq 0, \end{cases} \tag{14}$$

for all the neighboring i and j. From these inequalities, and assuming that $\Delta_\theta < \pi/2$, we have $\rho \leq |\cot(\Delta_\theta)|$. □

Next we characterize necessary and sufficient conditions for a linearized positive system to be row-diagonally dominant.

Lemma 1. *Suppose the linearized system (10) is positive. The system (10) is row-diagonally dominant if, and only if, the following inequality holds*

$$K_i + |B_{ii}| \geq (\sqrt{\rho^2+1} - 1) \sum_{j\in\mathcal{N}_i} |B_{ij}|. \tag{15}$$

Proof. Given the entries of A in (13) and Definition 1, the system (10) is row-diagonally dominant if, and only if,

$$|-K_i + B_{ii} + \sum_{j\in\mathcal{N}_i} B_{ij}| \geq \sum_{j\in\mathcal{N}_i} |-B_{ij}(\rho\sin(\theta_{ij}) + \cos(\theta_{ij}))|. \tag{16}$$

The proof follows by considering the worst-case phase-angle differences θ_{ij} that maximize the right-hand side term, i.e.,

$$\theta_{ij} = \underset{\theta\in[-\Delta_\theta,\, \Delta_\theta]}{\arg\max} \left(\rho\sin(\theta) + \cos(\theta)\right), \tag{17}$$

for all $(i,j) \in \mathcal{E}$. Since the system is positive from the inequalities in (14), we know that

$$\frac{\partial^2}{\partial\theta^2}\left(\rho\sin(\theta) + \cos(\theta)\right) \leq 0$$

holds for all the neighboring i and j. Hence, the solution to (17) can be obtained by solving the following equations

$$\begin{cases} 0 = \dfrac{\partial}{\partial\theta}\left(\rho\sin(\theta) + \cos(\theta)\right) \\ 1 = \sin(\theta)^2 + \cos(\theta)^2 \end{cases} \tag{18}$$

and verifying that its solution belongs to the feasible set $\theta \in [-\Delta_\theta,\ \Delta_\theta]$. In fact, the system of equations (18) is solved for $\theta^\star$ such that $\cos(\theta^\star) = 1/\sqrt{1+\rho^2}$. Note that $\theta^\star$ yields $\rho\sin(\theta^\star) + \cos(\theta^\star) = \sqrt{1+\rho^2} > 0$, which indicates that $\theta^\star$ satisfies the positivity constraints (14). Hence, since the linearized system is positive, we conclude that $\theta^\star$ belongs to the set $[-\Delta_\theta,\ \Delta_\theta]$, thus solving (17).

Considering the optimal value of (17), $\rho\sin(\theta^\star)+\cos(\theta^\star) = \sqrt{1+\rho^2}$, and noticing that the controller parameters K_i are positive and all the susceptance B_{ij} are negative, the proof concludes by rewriting the inequalities (16) as

$$K_i + |B_{ii}| + \sum_{j\in\mathcal{N}_i} |B_{ij}| \geq \sum_{j\in\mathcal{N}_i} \sqrt{\rho^2+1}|B_{ij}|. \tag{19}$$

□

These properties play important roles in the characterization of the attack impacts, and they are also used in analyzing the stability of the linearized system.

B. Stability of the power system

Next we establish the stability of the linearized system, using the positivity and row-diagonally dominance properties of the linearized system. Specifically, when the system is positive, the next result states the necessary and sufficient conditions for stability and then shows that row-diagonally dominance ensures stability.

Theorem 2. *Consider the linearized dynamics of the power system (10) and suppose the necessary and sufficient condition (12) from Theorem 1 is satisfied. Then the linearized system is positive and the following statements hold:*

1) *the system is asymptotically stable if and only if there exist positive scalars $\xi_i > 0$ such that the following inequality holds for all $i = 1, \ldots, n$:*

$$\xi_i|-K_i + B_i| > \sum_{j\in\mathcal{N}_i} \xi_j|-B_{ij}(\rho\sin(\theta_{ij}) + \cos(\theta_{ij}))|;$$

2) *the system is asymptotically stable if it is row-diagonally dominant, i.e., the following inequality holds for all $i = 1, \ldots, n$:*

$$|-K_i + B_i| > \sum_{j\in\mathcal{N}_i} |-B_{ij}(\rho\sin(\theta_{ij}) + \cos(\theta_{ij}))|.$$

Proof. Recalling that the entries of A are given by (13), the necessary and sufficient condition for stability follows directly

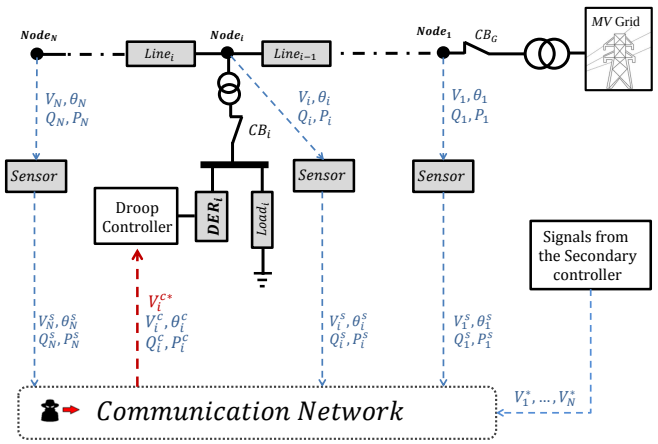

Figure 3. An inverter-based droop controller under a reference signal attack at bus i, where the adversary corrupts $V_i^{c\star}$.

from the positivity of the system and Proposition 1, i.e., the existence of a positive vector $\xi > 0$ such that $A\xi < 0$.

On the other hand, the sufficient condition for stability is obtained by considering $\xi_i = 1$ for all i and verifying that $A\mathbf{1} < 0$ can be rewritten as (16), given that τ_i and $\rho\sin(\theta_{ij}) + \cos(\theta_{ij})$ are positive and B_{ij} is negative. □

Remark 1. *Note that we may not have control on self-susceptance (B_{ii}) and it belongs to the interval $[0, \bar{B}_{ii}]$, so to be more conservative, the sufficient condition in Proposition 2 can be written as:*

$$K_i \geq \sum_{j\in\mathcal{N}_i} (\sqrt{\rho^2+1} - 1)|B_{ij}|. \tag{20}$$

Remark 2. *It could be interesting to characterize conditions on (10) under which V satisfies $|V - \mathbf{1}| < \delta$. This problem is related to the validity of (10), which assumes that V is positive. It also relates to how $V^{c\star}$ should be constrained so that the system is safe.*

V. Impact of Adversarial Actions

In this section, we consider different attack scenarios to the droop-controller and discuss preliminary results on their impact with respect to a linearized version of (9).

The following subsections follow a similar structure and each one considers a specific attack scenario. In particular, each subsection begins by describing the adversarial model and how it affects the droop-controller. Then, the impact of the attack is characterized based on properties of the linearized system, such as stability and input-output induced-norm. Such characterizations also aim at identifying which sets of attacked nodes yield possibly higher impacts, thus indicating which threats may pose a high risk to the system. The theoretical analysis is then complemented with numerical simulations of the attack scenarios in the nonlinear system (9).

A. Voltage reference attack

The present scenario considers an adversary that injects false-data into the communication network supporting the control system. In particular, we suppose that the reference signal of bus j is corrupted, as depicted in Fig. 3, so that

$$V_j^{c\star}(t) = u^a(t). \tag{21}$$

Hence, the corresponding control signal at bus j is given by

$$u_{V_j} = -K_j V_j^c \left(V_j^c - u^a(t)\right) - Q_j^c, \tag{22}$$

where the $u^a(t)$ is defined by the adversary. The impact of the attack is measured in terms of the resulting changes to the voltage magnitude at another bus $i \neq j$ in the network, i.e. V_i. The resulting linearized system can be expressed as

$$\begin{aligned} \dot{x}(t) &= Ax(t) + \tau_j^{-1} K_j e_j u^a(t) \\ y_i(t) &= e_i^\top x(t) \end{aligned} \tag{23}$$

where $A = -[\tau]^{-1}([K] + L(\theta))$ and $e_i \in \mathbb{R}^n$ is the i-th column of the n-dimensional identify matrix. In particular, we quantify the attack's impact as the maximum deviation of $y_i(t)$ caused by a corrupted reference $u^a(t)$ that is bounded as $|u^a(t)| \leq 1$. In fact, this metric corresponds to the $\mathcal{L}_\infty$-induced norm of (23). For power systems satisfying the conditions of Theorem 1 and Lemma 1, i.e., the system (23) is positive and stable, the following characterization of the worst-case attack naturally follows from Proposition 1.

Lemma 2. *Consider the linearized power system (10), which is assumed to be positive and asymptotically stable, and let $H_{ij}(s)$ be the transfer function of (23). The worst-case impact on node i of a reference attack on bus j, characterized as the $\mathcal{L}_\infty$-induced norm of (23), is given by $H_{ij}(0) = -\tau_j^{-1} K_j e_i^\top A^{-1} e_j = \tau_j^{-1} K_j [-A^{-1}]_{i,j}$.*

Such characterization of the worst-case impact can be leveraged to compare different attacks and identify scenarios with higher impact. In particular, supposing bus j is attacked, we are interested in assessing which other bus $i \neq j$ is most affected by the attack. That is, we seek to compute

$$i^\star = \arg\max_i H_{ij}(0) = \arg\max_i [-A^{-1}]_{i,j},$$

where the common factor $\tau_j^{-1} K_j$ has been omitted.

Although solving such problem would, in general, require the computation of all entries of $-A^{-1}$, specific power system topologies admit simpler solutions. Specifically, for power systems whose topology corresponds to a line graph, the following result establishes that the $\mathcal{L}_\infty$-induced norm $[-A^{-1}]_{i,j}$ decreases as the distance between i and j increases.

Theorem 3. *Consider a power system satisfying the conditions of Theorem 1 and Lemma 1, whose topology corresponds to a line graph. Furthermore, suppose the droop-controller at bus j is under a reference signal attack, being described by (22). Then the $\mathcal{L}_\infty$-induced norm of (23) is given by $H_{ij}(0) = \tau_j^{-1} K_j [-A^{-1}]_{i,j}$, which satisfies the monotonicity conditions*

$$\begin{aligned} [-A^{-1}]_{i,j} &> [-A^{-1}]_{i+1,j}, \ \forall j \leq i \\ [-A^{-1}]_{i,j} &> [-A^{-1}]_{i-1,j}, \ \forall j \geq i. \end{aligned} \tag{24}$$

Proof. Note that Theorem 1 and Lemma 1 imply that the power system (23) is positive and asymptotically stable, respectively. Hence, from Lemma 2, the $\mathcal{L}_\infty$-induced norm of (23) is given by $H_{ij}(0) = [-A^{-1}]_{i,j}$. Moreover, since the power system's topology is a line, the buses may be ordered so that the system matrix A is tridiagonal. Define the variables

$$\alpha_i = [-A]_{i,i}, \quad \beta_i = [-A]_{i,i+1}, \quad \varsigma_i = [-A]_{i+1,i},$$

which characterize the entries of the tridiagonal matrix $-A$. Assuming that $\beta_i \neq 0$ for all $i \leq N-1$, the inverse of A can be explicitly derived as [18, Theorem 2.1]

$$[-A^{-1}]_{i,j} = \begin{cases} (-1)^{i+j} \prod_{l=i}^{j-1} \beta_l \dfrac{\prod_{l=j+1}^{N} \phi_l}{\prod_{l=i}^{N} \delta_l} & \text{, if } j \geq i \\ (-1)^{i+j} \prod_{l=j}^{i-1} \varsigma_l \dfrac{\prod_{l=i+1}^{N} \phi_l}{\prod_{l=j}^{N} \delta_l} & \text{, if } j < i \end{cases}$$

with the convention that an empty product equals 1, where ϕ_i and δ_i are given by the recursions

$$\phi_i = \alpha_i - \frac{\beta_i \varsigma_i}{\phi_{i+1}}, \quad \phi_N = \alpha_N,$$
$$\delta_i = \alpha_i - \frac{\beta_{i-1}\varsigma_{i-1}}{\delta_{i-1}}, \quad \delta_1 = \alpha_1.$$

Hence, the conditions in (24) may be rewritten as

$$\begin{aligned} -\frac{\phi_{i+1}}{\varsigma_i} &> 1, \ \forall j \leq i \\ -\frac{\delta_{i-1}}{\beta_{i-1}} &> 1, \ \forall j \geq i. \end{aligned} \tag{25}$$

The proof follows through an induction argument, which makes use of the positivity and row-diagonally dominance properties of A. The induction argument for the second inequality of (24) is derived as follows. First we show that having $-\frac{\delta_{i-1}}{\beta_{i-1}} > 1$ for some $j \geq i$ implies that $-\frac{\delta_i}{\beta_i} > 1$ also holds. In fact, from the recursion of δ_i we have

$$\begin{aligned} \delta_i \geq -\beta_i - \varsigma_{i-1} - \frac{\beta_{i-1}\varsigma_{i-1}}{\delta_{i-1}} &= -\beta_i - \varsigma_{i-1}\left(1 + \frac{\beta_{i-1}}{\delta_{i-1}}\right) \\ &\geq -\beta_i > 0, \end{aligned}$$

where the first inequality follows from the positivity and the diagonally dominance properties of A, i.e., $\alpha_i = -[A]_{i,i} \geq [A]_{i,i+1} + [A]_{i,i-1} = -\beta_i - \varsigma_{i-1}$, while the hypothesis $-\frac{\delta_{i-1}}{\beta_{i-1}} > 1$ yields the second inequality. The induction argument is concluded by noting that $-\beta_i$ is positive and $-\frac{\delta_1}{\beta_1} = -\frac{\alpha_1}{\beta_1} \geq \frac{\beta_1}{\beta_1}$.

A similar proof holds for the first inequality of (24). □

Considering line graphs, using the results of Theorem 3, we conclude that the bus most affected by the attack at bus j, defined as $i^\star = \arg\max_i H_{ij}(0)$, corresponds to one of the neighboring buses of j, i.e., $i^\star = \arg \max_{i \in \{j-1,\, j+1\}} [-A^{-1}]_{i,j}$.

Numerical example: To illustrate the impact of the attack on the reference signal, we consider a radial 4-bus power system in island mode with identical power lines, loads, and inverters. The power system is characterized by (4) with the parameters $\rho = 0.5$, $B_{ij} = -0.2$, and $G_{ij} = -\rho B_{ij}$ for all edges $(i,j) \in \mathcal{E}$ and $B_{ii} = -0.001$ and $G_{ii} = \rho|B_{ii}|$ for all buses. The power inverters are modeled by (5) and (6) with parameters $\tau_i = 10^{-4}$ and $K_i = 0.2$ for all buses. Additionally, the phase-angle differences are constant throughout the simulation of the voltage dynamics and are given by $\theta_{12} = -0.11\text{rad}$, $\theta_{23} = 0.045\text{rad}$, and $\theta_{34} = -0.11\text{rad}$.

The system dynamics are described by the nonlinear differential equations (9), with the corresponding linearized dynamics characterized by (10) with

$$A = 10^{-4} \cdot \begin{bmatrix} -4.01 & 1.88 & 0 & 0 \\ 2.1 & -6.01 & 2.04 & 0 \\ 0 & 1.95 & -6.01 & 1.88 \\ 0 & 0 & 2.1 & -4.01 \end{bmatrix}.$$

Clearly, the system is positive and row-diagonally dominant. Since the diagonal entries A are negative, the system is also asymptotically stable.

Now consider the reference signal attack scenario where the voltage reference transmitted to bus 3 is corrupted by an adversary, which is modeled by (23). Following the discussion in this section, we seek to assess which buses, other than bus 3, are most affected by such attack. From Lemma 2, the worst-case impact of such attack on a given bus i in the network corresponds to $H_{i3}(0) = -K_3\tau_3^{-1} e_i^\top A^{-1} e_3$. In present example, the set of worst-case gains to buses 1, 2, and 4 are given by $H_{13}(0) = 0.09$, $H_{23}(0) = 0.19$, and $H_{43}(0) = 0.25$, respectively. As stated by Theorem 3, for line graphs, the largest worst-case impact takes place at one of the neighbors of bus 3, which here corresponds to bus 4.

The decrease of the impact as the distance to bus 3 increases is visible on the voltage trajectories of the nonlinear system under a reference attack on bus 3, as depicted in Fig. 4.

B. Voltage measurement routing attack

Here we consider an adversary that is able to redirect truthful data from its intended destination to another receiving bus in the network. In particular, we suppose that the adversary redirects the voltage measurement from bus j as if it were a measurement from bus i, which is captured by having

$$V_i^c = V_j^s = V_j.$$

The corresponding control signal under attack is described as

$$\begin{aligned} u_{V_i} &= -K_i V_j^s \left(V_j^s - V_i^{c\star}\right) - Q_i^c \\ u_{V_k} &= -K_k V_k^c \left(V_k^c - V_k^{c\star}\right) - Q_k^c, \ \forall k \neq i. \end{aligned} \tag{26}$$

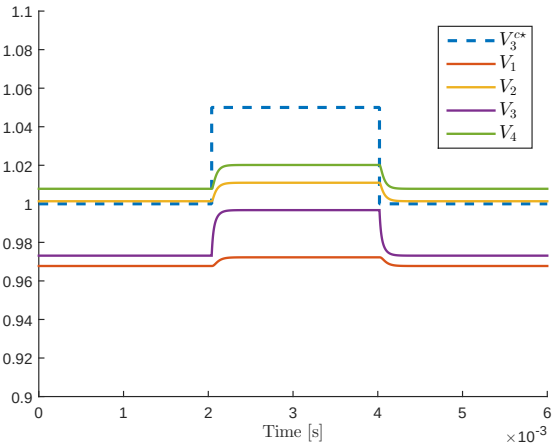

Figure 4. Trajectories of the voltage magnitudes under a reference signal attack at bus 3.

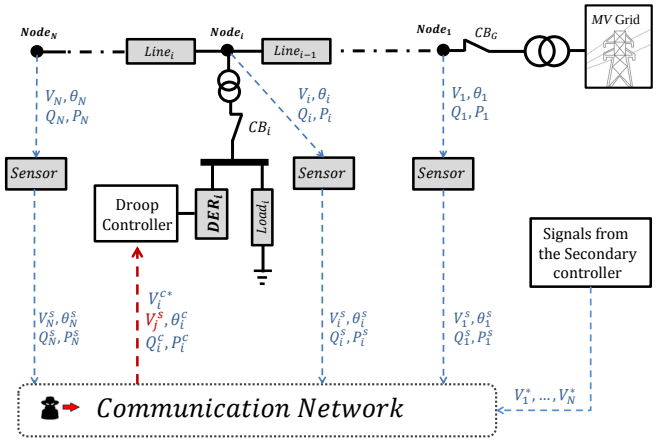

Figure 5. An inverter-based droop controller under a voltage measurement routing attack that feeds a measurement from bus j to bus i.

The resulting linearized system can be expressed as

$$\dot{x}(t) = \left(A - \tau_i^{-1} K_i e_i (e_j - e_i)^\top\right) x(t), \tag{27}$$

where the term $-\tau_i^{-1} K_i e_i (e_j - e_i)^\top x(t)$ can be interpreted as replacing the nominal feedback term $\tau_i^{-1} K_i V_i$ by the corrupted feedback $\tau_i^{-1} K_i V_j$ at bus i. In fact, such attack scenario can be rewritten as the following static output-feedback law

$$\begin{aligned} \dot{x}(t) &= \underbrace{(A + \tau_i^{-1} K_i e_i e_i^\top)}_{=\tilde{A}_i} x(t) + \tau_i^{-1} e_i u(t) \\ y_j(t) &= e_j^\top x(t) \\ u(t) &= -K_i y_j(t), \end{aligned} \tag{28}$$

where the matrix $\tilde{A}_i$ is independent of the control gain K_i.

Note that the closed-loop system under attack (27) is no longer positive, nor diagonally dominant, since we have $[A - \tau_i^{-1} K_i e_i (e_j - e_i)^\top]_{i,j} = -K_i < 0$ and $[A - \tau_i^{-1} K_i e_i (e_j - e_i)^\top]_{i,i} = [A]_{ii} + K_i$. As such, the results of Section IV may not be used to establish the stability of (27). In fact, the closed-loop system (27) may indeed be unstable for certain values of $K_i \geq 0$, as established by the following result.

Theorem 4. *Consider the power system under routing attack described by (27). There exists a control gain $K_i \geq 0$ for which the system is unstable if $\mathrm{dist}(j,i) \geq 2$, where $\mathrm{dist}(j,i)$ is the shortest length between buses i and j.*

Proof. The trivial case occurs when $\tilde{A}_i$ is not Hurwitz, for which $K_i = 0$ yields an unstable system. In the remaining of the proof, we suppose $\tilde{A}_i$ is Hurwitz. The proof follows from examining the root locus of the closed-loop system (28) with respect to the control gain $K_i > 0$. In particular, let r be the relative degree of the system, which also corresponds to the number of asymptotes of the root loci to which the closed-loop poles converge as $K_i > 0$ increases. Clearly, for $r \geq 3$ there exists at least one asymptote intersecting the complex right half-plane and we conclude that the system may become unstable for a sufficiently large gain K_i. To conclude the proof, we next argue that r is characterized as $r = \mathrm{dist}(j,i) + 1$.

Recall the definition of relative degree as the smallest integer $r \geq 1$ yielding a non-zero Markov parameter, i.e., $CA^{r-1}F \neq 0$. Given the particular structure of the feedback loop (28), this definition corresponds to the smallest integer for which $e_j^\top \tilde{A}_i^{r-1} e_i = [\tilde{A}_i^{r-1}]_{ji} \neq 0$ holds. Note that $\tilde{A}$ can be written as $\tilde{A}_i = -\mathcal{D}_i + \mathcal{A}$, where $\mathcal{D}_i$ is a diagonal positive definite matrix and $\mathcal{A}$ is a weighted adjacency matrix with positive edge-weights. Hence $\tilde{A}_i^k$ can be characterized as

$$\tilde{A}_i^k = \mathcal{A}^k + \sum_{l=0}^{k-1} \binom{k}{l} (-\mathcal{D}_i)^{k-l} \mathcal{A}^l. \tag{29}$$

Since the sparsity pattern of $\mathcal{A}^l$ is not altered by left-multiplying it with the diagonal matrix $(-\mathcal{D}_i)^{k-l}$, we conclude that $\min\{r > 0 \,|\, [\tilde{A}_i^{r-1}]_{ji} \neq 0\}$ is equal to $\min\{r > 0 \,|\, [\mathcal{A}^{r-1}]_{ji} \neq 0\}$. The remaining of the proof follows by using the non-negativity of $\mathcal{A}$ and Lemma 2.5 in [19], which states that there exists a path of length k between buses i and j if and only if $e_j^\top \mathcal{A}^k e_i > 0$. Since, by definition, $\mathrm{dist}(j,i)$ is the smallest integer such that $e_j^\top \mathcal{A}^{\mathrm{dist}(j,i)} e_i > 0$, we conclude that the system has relative degree $r = \mathrm{dist}(j,i) + 1$. □

Theorem 4 establishes the existence of a positive gain K_i for which the attacked system becomes unstable when $\mathrm{dist}(j,i) \geq 2$. Similar results were derived in [20] under the assumption that the open-loop system remains diagonally dominant, which does not hold for the present system.

Numerical example: Recall the example described in Section V-A and consider the measurement routing attack scenario where an adversary replaces the voltage measurement at bus 1 with the voltage measurement of bus 4, which is modeled by (27) with $i = 1$ and $j = 4$. The resulting closed-loop state matrix is

$$\tilde{A}_1 - K_1 e_1 e_4^\top = 10^{-4} \cdot \begin{bmatrix} -2.01 & 1.88 & 0 & -2 \\ 2.1 & -6.01 & 2.04 & 0 \\ 0 & 1.95 & -6.01 & 1.88 \\ 0 & 0 & 2.1 & -4.01 \end{bmatrix},$$

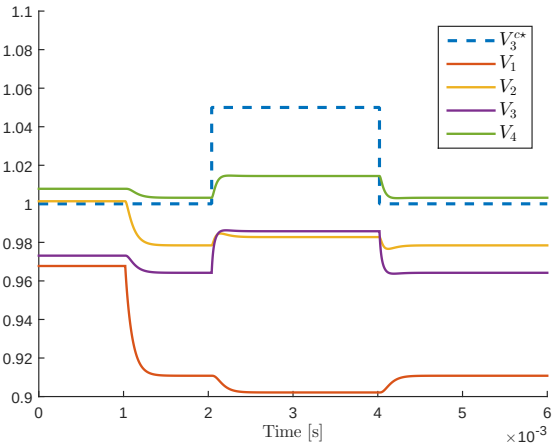

Figure 6. Trajectories of the voltage magnitudes under a voltage measurement routing attack that feeds a measurement from bus 4 to bus 1, followed by a reference change at bus 3.

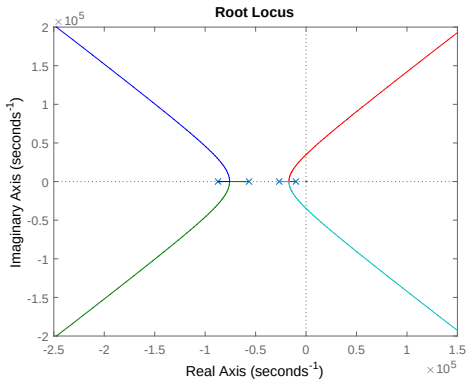

Figure 7. Root-locus of the system (28) with respect to $K_1 \geq 0$.

which is clearly not diagonally dominant, nor positive. Despite stability, the lack of such properties leads to contradictory behaviors, as illustrated by the response to a step-change in one reference, depicted in Fig. 6. Despite the increase in the reference signal, bus 1 further decreased its voltage.

As stated in Theorem 4, since the distance between buses 1 and 4 is greater than 1, there exists a gain $K_1 \geq 0$ for which the system under attack becomes unstable. This is illustrated through the corresponding root-locus depicted in Fig. 7.

VI. Conclusion

In this paper, we studied the properties of a voltage droop control scheme in interconnected microgrids under adversarial actions. First the power system dynamics under nominal operation were analyzed, and conditions ensuring relevant system properties, including stability, were derived. Then, two attack scenarios were discussed, where the adversary is able to manipulate the measurement data and reference signals received by the voltage droop controllers. Each attack scenario admits multiple instances, depending of which set of nodes are attacked. The potential impact of different instances of each scenario were compared using control-theoretic tools, which provides a basis to identify high-risk attack instance in each scenario. Our methodology was illustrated on a line network through numerical examples.

References

[1] N. Hatziargyriou, H. Asano, R. Iravani, and C. Marnay, "Microgrids," *Power and Energy Magazine, IEEE*, vol. 5, no. 4, pp. 78–94, July 2007.

[2] F. Shahnia, R. P. Chandrasena, S. Rajakaruna, and A. Ghosh, "Primary control level of parallel distributed energy resources converters in system of multiple interconnected autonomous microgrids within self-healing networks," *IET Generation, Transmission & Distribution*, vol. 8, no. 2, pp. 203–222, 2014.

[3] G. Andersson, P. Esfahani, M. Vrakopoulou, K. Margellos, J. Lygeros, A. Teixeira, G. Dan, H. Sandberg, and K. Johansson, "Cyber-security of scada systems," in *Innovative Smart Grid Technologies (ISGT), IEEE PES*, Jan 2012, pp. 1–2.

[4] Y. Liu, M. K. Reiter, and P. Ning, "False data injection attacks against state estimation in electric power grids," in *16th ACM Conference on Computer and Communications Security*, 2009.

[5] H. Sandberg, A. Teixeira, and K. H. Johansson, "On security indices for state estimators in power networks," in *First Workshop on Secure Control Systems, CPSWeek*, Stockholm, Sweden, Apr. 2010.

[6] G. Hug and J. Giampapa, "Vulnerability assessment of AC state estimation with respect to false data injection cyber-attacks," *Smart Grid, IEEE Transactions on*, vol. 3, no. 3, pp. 1362–1370, Sept 2012.

[7] K. C. Sou, H. Sandberg, and K. H. Johansson, "Electric power network security analysis via minimum cut relaxation," in *50th IEEE Conference on Decision and Control*, Dec. 2011.

[8] L. Xie, Y. Mo, and B. Sinopoli, "False data injection attacks in electricity markets," in *First IEEE International Conference on Smart Grid Communications*, 2010.

[9] A. Teixeira, H. Sandberg, G. Dán, and K. H. Johansson, "Optimal power flow: closing the loop over corrupted data," in *American Control Conference*, 2012.

[10] O. Kosut, L. Jia, R. Thomas, and L. Tong, "Malicious data attacks on smart grid state estimation: Attack strategies and countermeasures," in *First IEEE International Conference on Smart Grid Communications*, 2010.

[11] O. Vukovic, K. C. Sou, G. Dán, and H. Sandberg, "Network-aware mitigation of data integrity attacks on power system state estimation," *IEEE Journal on Selected Areas in Communications*, vol. 30, no. 6, pp. 1108–1118, 2012.

[12] Y. Isozaki, S. Yoshizawa, Y. Fujimoto, H. Ishii, I. Ono, T. Onoda, and Y. Hayashi, "On detection of cyber attacks against voltage control in distribution power grids," in *Smart Grid Communications, IEEE International Conference on*, Nov. 2014, pp. 842–847.

[13] A. Teixeira, G. Dán, H. Sandberg, R. Berthier, R. Bobba, and A. Valdes, "Security of smart distribution grids: Data integrity attacks on integrated Volt/VAR control and countermeasures," in *American Control Conference*, June 2014, pp. 4372–4378.

[14] J. W. Simpson-Porco, F. Drfler, and F. Bullo, "Synchronization and power sharing for droop-controlled inverters in islanded microgrids," *Automatica*, vol. 49, no. 9, pp. 2603 – 2611, 2013.

[15] J. Simpson-Porco, F. Dorfler, and F. Bullo, "Voltage stabilization in microgrids via quadratic droop control," in *Decision and Control (CDC), IEEE 52nd Conference on*, Dec 2013, pp. 7582–7589.

[16] J. Schiffer, R. Ortega, A. Astolfi, J. Raisch, and T. Sezi, "Conditions for stability of droop-controlled inverter-based microgrids," *Automatica*, vol. 50, no. 10, pp. 2457–2469, 2014.

[17] A. Rantzer, "Distributed control of positive systems," in *Decision and Control and European Control Conference (CDC-ECC), 50th IEEE Conference on*, Dec 2011, pp. 6608–6611.

[18] C. M. da Fonseca and J. Petronilho, "Explicit inverses of some tridiagonal matrices," *Linear Algebra and its Applications*, vol. 325, no. 1–3, 2001.

[19] J. B. Hoagg and D. S. Bernstein, "On the zeros, initial undershoot, and relative degree of lumped-mass structures," in *American Control Conference*, June 2006, pp. 394–399.

[20] J. A.Torres and S. Roy, "Stabilization and destabilization of network processes by sparse remote feedback: Graph-theoretic approach," in *American Control Conference*, June 2014, pp. 3984–3989.